Articles   Directorate of Academic Affairs

2016-5

The Evaluation and Implementation of Magnetic Fields for Large Strain Uniaxial and Biaxial Cyclic Testing of Magnetorheological Elastomers.

Dave Gorman
Technological University Dublin, david.gorman@tudublin.ie

Niall Murphy
Technological University Dublin, niall.murphy@tudublin.ie

Ray Ekins
Technological University Dublin, ray.ekins@tudublin.ie

See next page for additional authors

Follow this and additional works at: https://arrow.tudublin.ie/diraaart

Part of the Engineering Physics Commons, and the Materials Chemistry Commons

Authors

Dave Gorman, Niall Murphy, Ray Ekins, and Stephen Jerrams

Title: The evaluation and implementation of magnetic fields for large strain uniaxial and biaxial cyclic testing of Magnetorheological Elastomers.

Authors and Affiliations

Dave Gorman, Niall Murphy, Ray Ekins, and Stephen Jerrams

Dublin Institute of Technology Dublin 1

Corresponding Author Dave Gorman david.gorman@dit.ie

Abstract

Magnetorheological Elastomers (MREs) are "smart" materials whose physical properties are altered by the application of magnetic fields. In previous studies the properties of MREs have been evaluated under a variety of conditions, however little attention has been paid to the recording and reporting of the magnetic fields used in these tests [1]. Currently there is no standard accepted method for specifying the magnetic field applied during MRE testing. This study presents a detailed map of a magnetic field applied during MRE tests as well as providing the first comparative results for uniaxial and biaxial testing under high strain fatigue test conditions. Both uniaxial tension tests and equi-biaxial bubble inflation tests were performed on isotropic natural rubber MREs using the same magnetic fields having magnetic flux densities up to 206mT. The samples were cycled between pre-set strain limits. The magnetic field was switched on for a number of consecutive cycles and off for the same number of following cycles. The resultant change in stress due to the application and removal of the magnetic field was recorded and results are presented.

Keywords

Magnetorheological Elastomers; Magnetic fields; Uniaxial tension; Biaxial bubble inflation; Natural Rubber; Fatigue

1. Introduction

Magnetorheological Elastomers (MREs) are classified as smart materials that undergo a change in their physical properties which is observed as an increase in modulus when a magnetic field is applied to an MRE [2]. The increase in the modulus is caused by the ferromagnetic particles which are added to the elastomer during the curing process, tending to align with the applied magnetic field. The alignment occurs because the applied field results in dipole-dipole interactions between the particles which move to screen each other from the field and adopt a minimum energy configuration [3].

All MREs consist of two key components, the elastomeric matrix and ferromagnetic particles. MREs can also be classified into two broad groups; isotropic and anisotropic. Isotropic MREs contain an almost homogeneous distribution of magnetic particles whereas anisotropic MREs contain aligned particle chains. These chains are formed by the application of a magnetic field during the curing process [4]. Once the matrix has been cured, the particle mobility is reduced and the aligned chains remain in position. MREs with aligned particles normally exhibit a greater magnetorheological effect than isotropic MREs when the magnetic field is applied parallel to the direction of the particle chains [4].

To date, MRE testing has predominantly been carried out on uniaxially loaded samples [5]. However the data provided on the magnetic fields prevents an accurate replication of many

tests as the magnetic field is stated as uniform in both flux density and direction over the entire sample volume. The greater the distance between the magnetic poles, the less accurate this statement becomes. [1, 5, 6].

The focus of this research is twofold. Firstly to provide an accurate representation of a magnetic field applied to MRE samples during both uniaxial tensile and biaxial bubble inflation fatigue tests and secondly, to provide the first comparative results between uniaxial and biaxial cyclic loading testing for an MRE exposed to the same magnetic field under both test modes.

2. Apparatus and Materials

2.1 Magnetorheological Elastomers

The MRE samples used in all tests reported in this paper consist of isotropic carbon black filled 1.65% (volume per volume) vulcanised natural rubber with 18.3% (volume per volume) iron particles Previous studies [2-4, 7-9] have focused on soft elastomer matrix (silicone or urethane) based MREs as these elastomers have a greater particle mobility and hence undergo a greater increase in modulus when a magnetic field is applied. Other studies [10-12] have focused on natural rubber based MREs as their superior physical (modulus) and fatigue properties offer potential applications such as Adaptive Tuned Vibration Absorbers (ATVAs) [11].

As the primary goal of this study is to specify a magnetic field and evaluate its effect on two separate test methods, variations in test results due to sample manufacture or orientation (particle chains in anisotropic samples) were minimised by use of isotropic samples produced by a replicable commercial production method.

The samples used in the uniaxial tensile strength tests were 70mm x 20mm x 1mm strips with the direction of extension being in the direction of the 70mm length. For the biaxial bubble inflation tests, discs of 50mm diameter and 1mm thickness were used.

2.2 Electromagnetic Array

All magnetic fields applied in this study to both the uniaxial and biaxial tests were generated by the same electromagnetic array. A prototype of this array was described in a previous study by the authors [1] but has since undergone further modifications to increase the flux density. An FEA model of this modified array is shown in figure 1. Electromagnets have a number of advantages and disadvantages when compared with permanent magnets. The main advantage offered by permanent magnets is that they do not require a constant input of power to maintain the magnetic field [13].This is offset by the fact the an electromagnetic array allows for the field to be turned on and off during a test so that data can be collected with and without the magnetic field applied for the same sample during a single test. The same tests can be repeated using fields of different flux density by altering the current supplied to the coils.

The magnetic array discussed here uses low carbon steel rods of 50mm for the magnetic core and magnetic circuit. This arrangement is shown in the FEA model (FEMM4.2 modelling software [14]) in figure 1 and 3D schematic in figure 2.
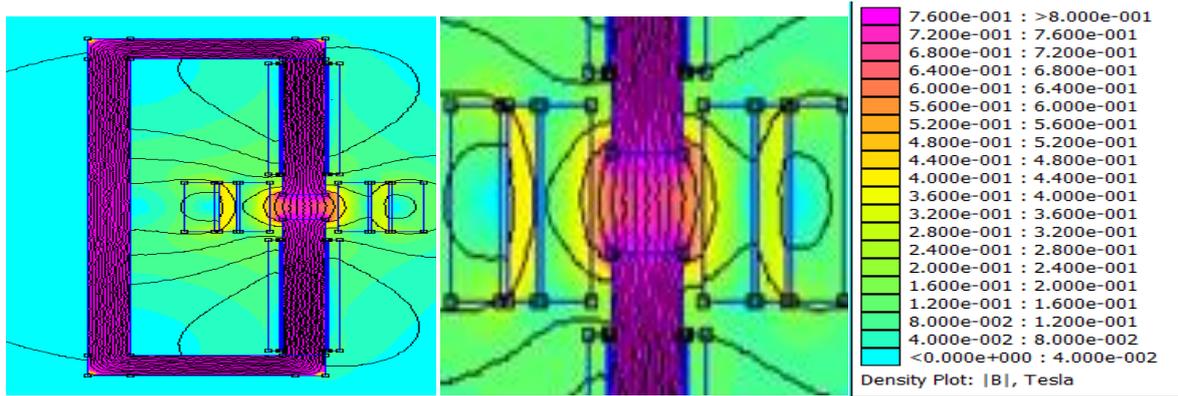
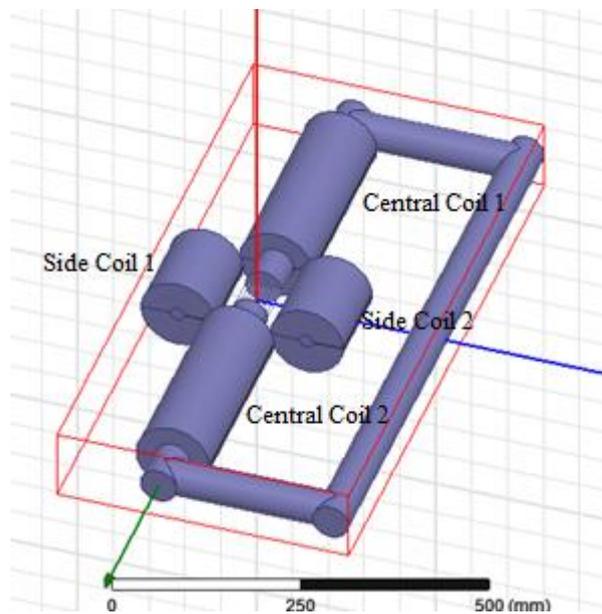Fig 1. 2D FEA model of the array used during testing

Fig 2. 3D schematic showing position of electromagnets

The array consists of four 1500 turn electromagnets with current flowing in one direction for the two central coils and in the opposite direction for the two side coils to give the same north and south pole arraignment as the open access Halbach array used in NMR imaging by Hills [15]. The magnetic circuit is a constant 50mm diameter for the entire circuit length to maximise the flux density of the field which can be applied to the samples. The updated array incorporates the same cooling system power supply and side coils of the prototype [1].

3 Testing methods

3.1 Uniaxial tensile fatigue tests

Uniaxial tensile fatigue tests were performed on 70mm x 20mm x 1mm isotropic natural rubber MREs with the strain applied along the 70mm length of the sample (ie zero strain l_0=70mm) and the cross sectional area of the sample being 20mm^2. These tests were conducted on a Zwick uniaxial tensile test machine.

All tests carried out were constant strain amplitude tests. The stress was calculated as true stress from the load cell output. $\sigma_{true} = \frac{F\lambda}{A}$ where σ_{true} is the true (Cauchy) stress, F is the force on the load cell, A is the initial cross sectional area of the sample, and λ is the stretch ratio (strain+1). All modulus values reported in this study are for $E_{true} = \frac{\sigma_{true}}{\varepsilon}$ where ε is the strain.

The magnetic fields were field was applied perpendicular to the strain direction for all uniaxial tests. Each test consisted of 500 cycles at 1Hz with the field switched off for the first 50 cycles and being switched on at the 50th cycle for the next 50 cycles before being switched off at the 100th cycle. This off/on switching of the magnetic field continued until the test ended with the field in the on position for cycles 450 to 500.

3.2 Equi-biaxial bubble inflation tests.

The equi-biaxial tests were carried out on the DYNAMET equibiaxial bubble inflation test machine developed in the Dublin Institute of Technology by Murphy et al [16, 17] and further developed by Johnson et al [18]. Both stress (using the pressure, radius of curvature and strain) and strain are recorded directly using a vision system. Modulus is calculated in the same manner as in the uniaxial tests where $E_{true} = \frac{\sigma_{true}}{\varepsilon}$.

The DYNAMET's vision system comprises two CMOS (complementary metal-oxide semiconductor) cameras which recorded values in one axis of strain only. The magnetic field runs parallel to the applied strain in the axis for which the data is being recorded for all biaxial tests. Each test consisted of 150 cycles 0.2Hz with the field initially in the off position for the first 90 cycles and being switched on at the 90th cycle. The field is alternately turned on and off for all subsequent sets of 20 cycles with the test ending with the field in the on position for cycles 130 to 150. The bubble inflation tests were conducted at a lower frequency than the uniaxial tests to increase the number of data points per cycle as they are obtained from the real time vision control system.

3.3 Characterization of the magnetic field

Before any tests were carried out, the magnetic field was mapped using a Lake Shore model 460 3-axis Gaussmeter and 3 axis Hall probe with no sample present. The Hall probe is capable of measuring the field in the x y and z axes to an accuracy of ±0.1mT. It consisted of three orthogonally mounted Hall generators in a probe structure with a separate output for each axis on the Gaussmeter which allows field direction to be calculated. The centre point of the air gap in the electromagnetic array was designated as the datum point (0,0,0). The array and Hall probe were mounted on a xyz translation stage (milling machine) and the position of the probe could be measured to an accuracy of ±0.01mm in each axis. Figure 3 shows the array on the test bed during mapping of the flux density.

Fig 3. 3 axis experimental set up to map magnetic field

The magnetic flux density of the field was mapped by moving the hall probe 5mm in one axis to a precision of ± 0.05mm and recording the values on the Gaussmeter. The field was mapped in the x y plane with a fixed z value and when this map was completed the probe was moved in the z axis and another x y plane map was produced. The field was mapped for +/- 25mm in the x and y axis and +/-20mm in the z axis to provide a measure of the field over the sample volume without the presence of a magnetic sample. All flux density values quoted are for the datum point (0,0,0) with no sample present unless otherwise stated, as the presence of a sample will alter the magnetic flux density.

4 Results

4.1 Magnetic field mapping results

A previous study on a prototype version of the electromagnetic array used in this study [1] showed that there was a substantial difference between the field calculated by the FEA software and the actual values recorded by the Gaussmeter in the air gap between the pole pieces of the electromagnetic array. Despite this difference in the flux density values, the 2D FEA modelling provided useful information in field mapping and design for saturation current values, field line direction and the profile of the flux density uniformity.

The results presented in figure 4 show the recorded flux density, at the centre point of the array for a range of currents without the presence of a sample. This shows the range of flux densities which can be applied to a sample during both uniaxial and biaxial testing up to a maximum flux density of 206mT. It is also clear from figure 3 that the cores of the electromagnets are approaching saturation illustrated by the drop in the rate of increase of flux density as the current is increased.
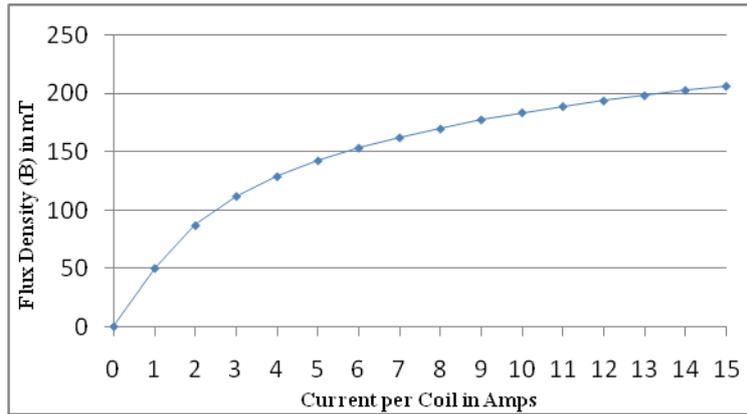
Fig 4 Flux Density at centre of air gap v Current per Coil

The graph in figure 5 shows the effect that the presence of an MRE sample can have on the overall flux density. To record this effect a sample which was used for a bubble inflation test was punctured at its centre and the sample was placed over the Hall probe and the same tests were repeated. This shows an increase of 29mT, from 206 mT to 235mT, in the flux density for the maximum flux density value at the centre of the sample.
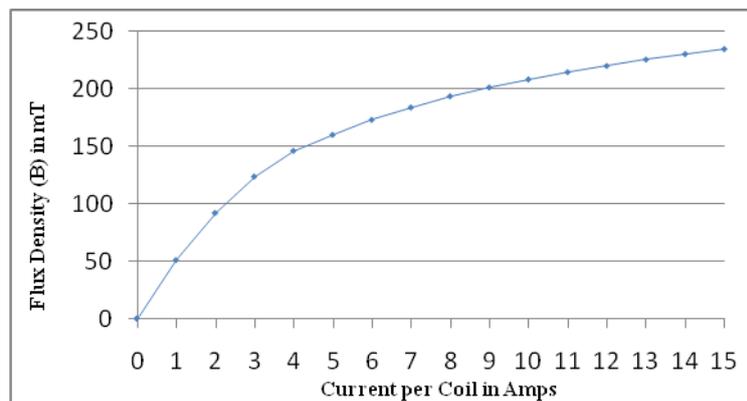

Fig 5 Flux Density at centre of air gap v Current per Coil with MRE sample present

As different samples contain varying amounts and distributions of iron particles, they will have a different effect on the magnetic field; therefore the only field which can be stated as the same for each test is that which is recorded without the presence of the sample. From the data presented in figures 4 and 5, the relative permeability (μ_r) of the MRE sample can be calculated by dividing the flux density recorded with the sample present by the flux density without the sample. This results in a μ_r value of 1.14±0.03 for flux densities without the sample above 130mT. For flux densities below this value the relative permeability is lower at 1.02, 1.06, and 1.11, for the 1, 2, and 3 amps per coil flux density values shown in figure 3.

To determine the uniformity of the magnetic field, the flux density was recorded for the array in five xy planes with differing values of z. The results are shown in figures 6. With this data in conjunction with the sample position it is possible calculate the flux density range at the point which the MRE experiences maximum strain. This information is presented in table 1 for the z axis and table 2 for the (x,y) planes. All the graphs in figure 6 are recorded at a current of 7amps per coil in the array
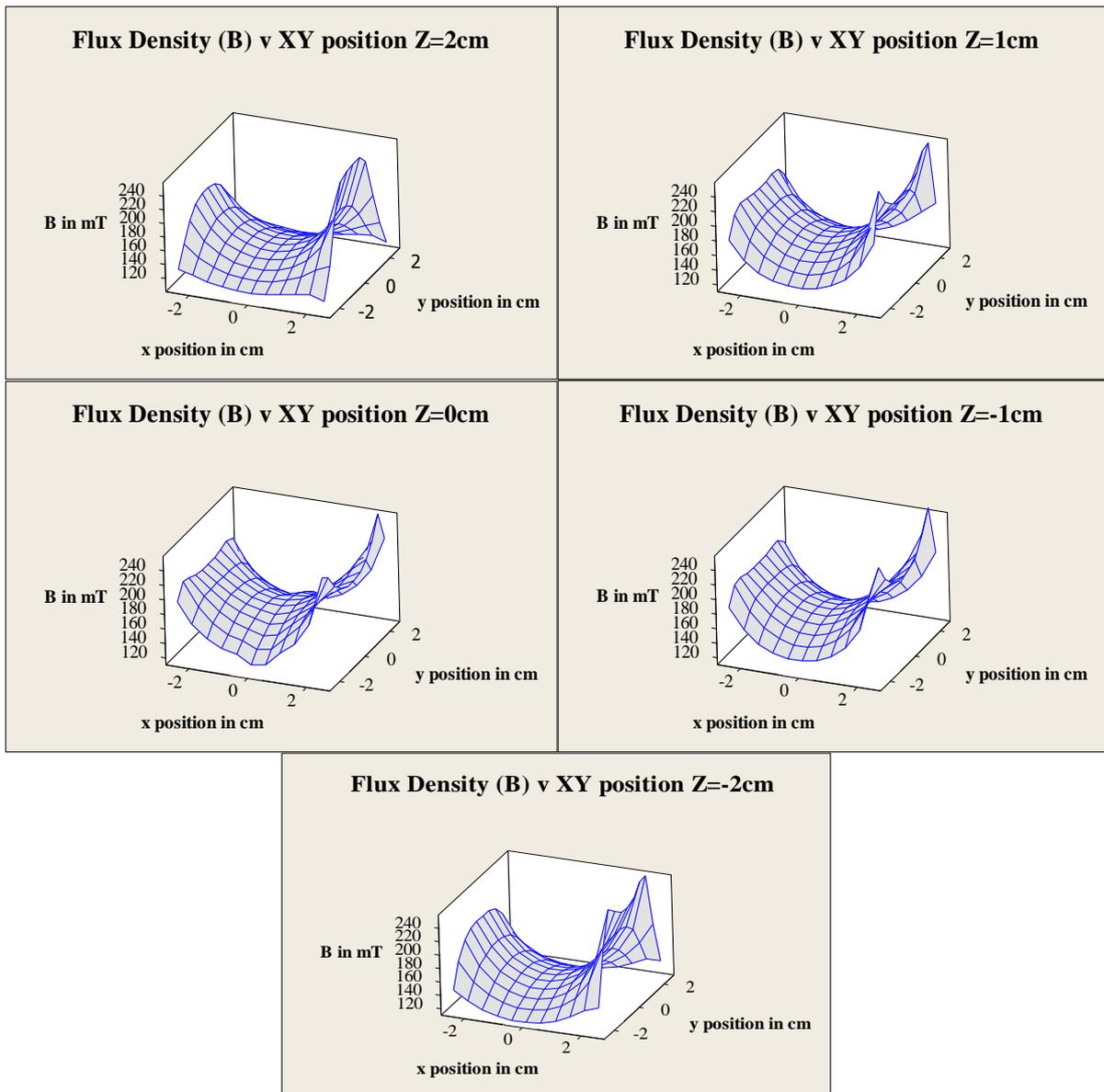
Fig 6 xy plane plots of flux density at different z values

Table 1 uniformity of flux in z axis

Z value in mm relative to centre	Flux Density in mT
20	137.1
10	155.3
0	161.3
-10	156.6
-20	140.0

The data in table 1 shows a measure of the flux density of the centre points $(x,y) = (0,0)$ with differing values of z taken from the graphs presented in figure 5. This shows how the applied flux density varies along a 40mm length of a uniaxial tensile test sample with a difference in

flux density of 15% ($\frac{161.3 - 137.1}{161.1} \times 100$) from the centre field value to its lowest point at a z displacement of 20mm

The data in table 2 shows a measure of the flux density of the central z = 0 plane from the graphs presented in figure 5. This shows the change in the flux density in the xy planes with a difference of +9.5% and -4.8% from the centre field value at its maximum and minimum points in the 400mm^2 area. This illustrates the non-symmetric saddle shaped plot of the flux density profile shown in figure 5. Therefore any flux value stated in this report has a maximum error of +9.5% and -4.8% on the stated figure, or a 14.3% change in the flux density from max to min over this area. The field direction over this area was calculated by comparing the flux density in the x axis B_x with the total flux density B_t at the each point. These agreed to within 0.1mT for all points in the two tables showing the field has a uniform direction in the x axis for the region of interest for all tests. The central area of these planes is the region in which the vision system records its data for bubble inflation tests which for a stretch ratio of 1.4 (strain 0.4) would cover a maximum area of 70mm^2 centred on the pole of an inflated bubble sample. This gives a maximum variation in flux density over the region measured by the vision system of 5.0%.

Table 2 uniformity of flux in xy plane

(x,y) value mm relative to centre	Flux Density in mT
(0,0)	161.3
(0,10)	159.5
(0,-10)	153.5
(10,0)	176.6
(10,10)	172.7
(10,-10)	173.8
(-10,0)	167
(-10,10)	161.5
(-10,-10)	163.8

These results show that there is a variation of magnetic flux density being applied throughout the test sample volume. However, this is a more accurate representation of the actual flux density than that usually reported ie. a single value of flux density at a point. The deviation reported here will always be a characteristic of magnetic fields in air due to the $1/r^2$ relationship [19].

4.2 Material Testing Results

All tests on MREs reported in this study were carried out under conditions of cyclic loading between fixed strain limits (ΔL). These tests were chosen over load control tests as the

application of the magnetic field causes an increase in the modulus of the MRE and such a change is easily detectable on a load cell for uniaxial tests and on the calculated stress measurements for biaxial tests. The MR properties of the material were evaluated by varying the applied magnetic flux density while maintaining the same strain control limits for the test samples, during both uniaxial and biaxial tensile fatigue tests.

Initial uniaxial tests were carried out at low strain amplitude values to evaluate if the test procedures were sufficiently sensitive to detect the MR effect as the effect is greatest with low strain cycling (particles closer together for screening effects) and maximum flux applied. These tests were carried out on uniaxial samples cycled between strain limits of 0.04 and 0.08 at 1Hz. The modulus was calculated for each data point recorded in the cycle. No field was applied for cycles 10-60. The field was then applied for cycles 60-110 and alternated between off and on for every subsequent 50 cycles throughout the test. The graphs in figures 7-8 show how the MR effect is calculated and presented in different formats. Figure 6 shows the modulus of the sample plotted against the cycle number. The graph shows a stepped instantaneous increase in modulus when the field is applied which is reversed when the field is removed. For figure 7 only the final 200 cycles were taken as the early cycles show diminishing maximum stress values due to the Mullins effect [20]. Figure 7 shows the average modulus calculated from all points in a single cycle for each cycle (Blue line) and the average using all points in the 50 cycle blocks (red line). The error bars on the red line are calculated using the standard error formula and shows the error on the modulus (the modulus reported is the mean modulus value and the standard error calculates the statistical error on the mean). Standard stress strain graphs were also produced to show the MR effect and are shown in figures 8 10 12 and 14. Figure 8 represents the final 100 cycles from figure 7. This was calculated by taking the average stress in a fixed strain range for the points in the 50 cycles with the field off (blue) and for the subsequent 50 cycles with the field on (red). The stepped increase in modulus, visible at the 360th cycle on the x axis, is from 1.325MPa to 1.413MPa. This is an increase of approximately 6.5% in the average modulus of the 50 cycle block. This corresponds with the field being switched on at cycle 360.
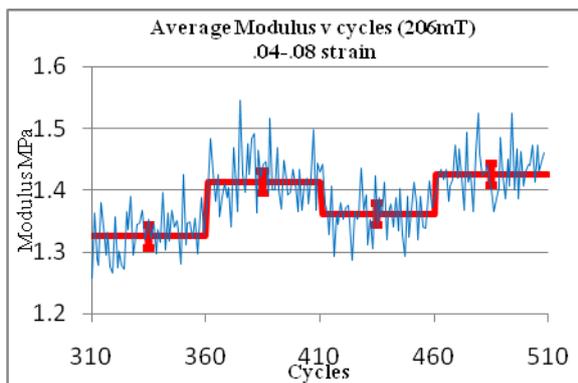

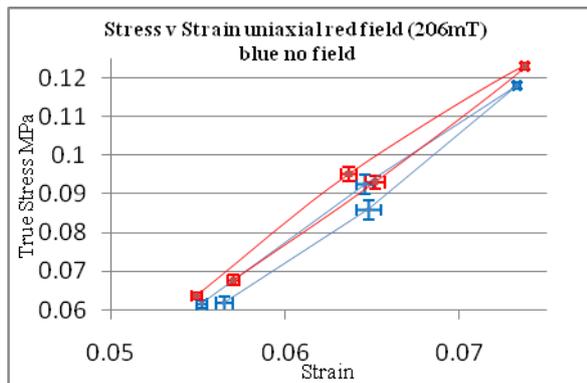Fig **7** Average Modulus v Cycles uniaxial data flux density 206mT   Fig 8 Stress Strain uniaxial data flux density 206mT

The tests were repeated with an applied flux density of 112mT and the results are shown in figures 9 and 10. While there is still a detectable increase at cycle 360 when the magnetic field is switched on from 1.242MPa to 1.268MPa which corresponds to an increase in modulus of 2.1%, it is less than the effect observed in figures 6 and 7. By comparing figures 6 and 8 it is clear that the MR effect depends on the magnitude of the applied flux density as would be expected.
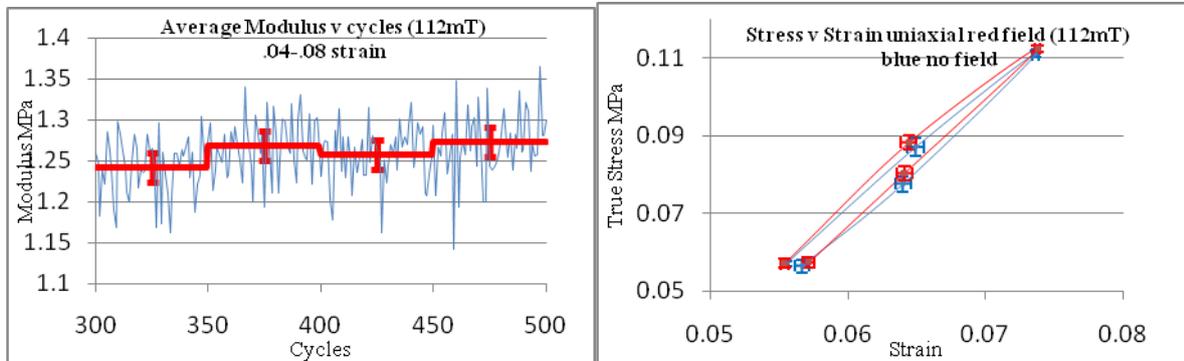

Fig 9 Average Modulus v Cycles uniaxial data flux density 112mT   Fig 10 Stress Strain uniaxial data flux density 112mT

Samples were also tested under biaxial bubble inflation conditions between strain values of 0.1 and 0.4 and cycled at 0.2Hz and the effect of varying the applied magnetic flux was investigated. Figure 11 shows modulus versus cycles for the final 80 cycles for a bubble inflation test with the magnetic field alternatively switching on and off for blocks of 20 consecutive cycles. This shows the average modulus calculated from all points in a single cycle for each cycle (Blue line) and the average using all points in the 20 cycle blocks (red line). The error bars on the red line are calculated using the standard error formula and shows the statistical error on the modulus. Standard stress-strain graphs were also produced to show the MR effect. Figure 15 represents the final 40 cycles from figure 10 and was produced by taking the average stress in a fixed strain range for the points in a 20 cycle block with the field off (blue) and for a subsequent 20 cycle block with the field on (red). The increase in modulus is more obvious when displayed as an increase in the average modulus versus cycles rather than the standard stress strain graphs.
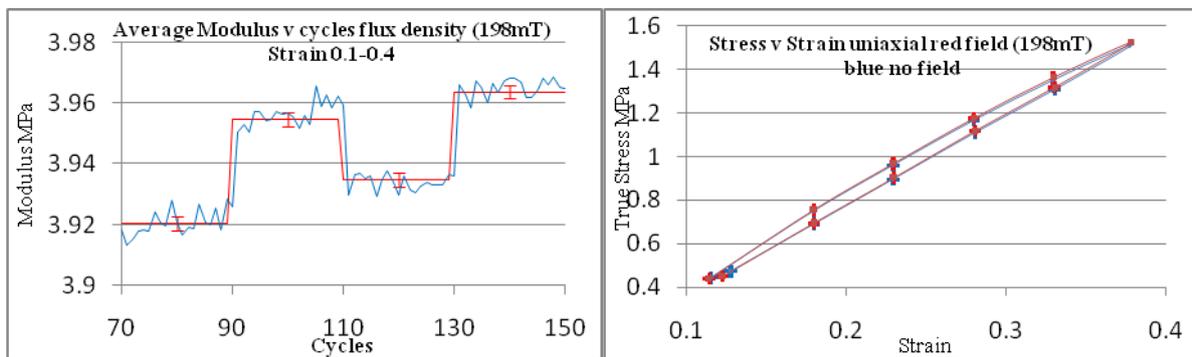

Fig 11 Average Modulus v Cycles biaxial data flux density 198mT   Fig 12 Stress Strain biaxial data flux density 198mT

The increase in the modulus recorded at cycle 90 is from 3.92MPa to 3.954MPa corresponding to an increase of 0.8% in the block average modulus. It is impossible to directly compare biaxial results to those from uniaxial test data as although the same

strain/stretch ratio is applied, recorded stress and therefore the calculated modulus for the biaxial sample will be higher as it is stretched in two perpendicular directions simultaneously and has a greater effective strain than the equivalent uniaxial strain/stress ratio. Figures 13 and 14 show similar tests to those in figures 11 and 12, repeated with an applied flux density of 112mT. The increase in the modulus of the sample at cycle 130 is from 3.764MPa to 3.771MPa or approximately 0.13%. Again as was the case in uniaxial testing this shows the MR effect is proportional to the flux density applied to the sample. The drop recorded in the average modulus from cycles 90-110 compared with cycles 70-90 is due to continued stress softening of the sample. There is a change in the average modulus from cycles 70-90 and cycles 90-110 but it is statistically insignificant due to the overlap of the error bars, however an increase in modulus when the magnetic field is applied is visible at cycle 130. This reduction in the MR effect to statistically insignificant values corresponds with uniaxial results and is to be expected at reduced field strengths.
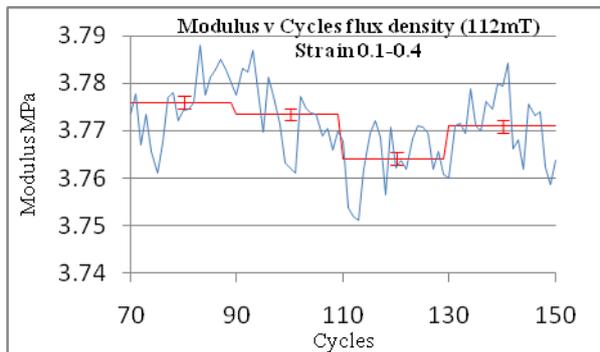

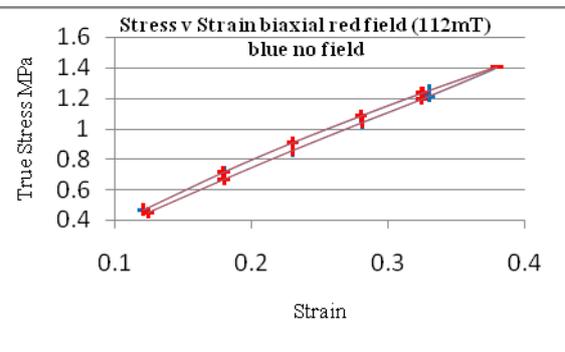Fig 13 Average Modulus v Cycles biaxial data flux density 112mT   Fig 14 Stress Strain biaxial data flux density 112mT

5 Conclusions

5.1 Magnetic field reporting.

The largest difficulty in replicating previously published MRE tests is the absence of a standard method of reporting the details of the magnetic field applied to the sample. A single flux density value is insufficient information to obtain a detailed understanding of the applied magnetic field and allow for an accurate replication of the test conditions. Therefore it is necessary for an agreed standard method for describing the magnetic field applied to any testing of an MRE. The following standard for detailing the applied magnetic field for an MRE test is proposed.

1) A magnetic flux line diagram of the applied field (figure 1) is necessary as the direction of the applied flux with respect to force and particle chains (anisotropic MREs only) can have a different effect on the sample. [4]
2) A detailed map of the flux density over the entire volume between the poles is required. As can be seen from the results in figure 6 and tables 1-2, small changes in the position of the probe result in a change in the measured flux density. The map should be of the actual measured field as current magnetic models may not be sufficiently accurate to model the magnetic flux in the air gap between the poles which is where the MRE sample will be placed. The flux density map also needs to be verified by physical measurement [1].
3) The measurement of the flux density should be carried out without the presence of the sample as the results from figures 4 and 5 show the presence of the sample will alter

the flux density values. The only field value which can be verified when applied to all samples is the field recorded without a sample present.

4) When stating a flux density value, the location at which that value was recorded needs to be stated i.e. the centre point of the air gap and this should be the midpoint about which the bubble pole traverses in the case of a bubble inflation sample.

5.2 Material testing results.

From the results shown in figures 7-14 it is clear than an electromagnetic array can be designed and constructed which is suitable for the testing of MREs under high strain uniaxial loading conditions and the same array can also be used in biaxial bubble inflation tests of MREs. This array allows for the comparison of the results between the two different test methods as the only difference between them will be due to the actual test methods themselves.

In both test methods a clear MR effect is visible for flux densities in the region of 200mT for high modulus (hard) natural rubber isotropic MREs. A reduced MR effect can be detected for fields above 100mT for both uniaxially and biaxially loaded samples. Therefore it can be concluded that as the MR effect can be detected in isotropic natural rubber MREs using this method, softer isotropic and anisotropic MREs can also be evaluated as they all exhibit higher MR effects than for isotropic natural rubber based MREs [10]. However, the increase in the modulus with the magnetic field applied is lower than the increases reported by McIntyre [21] [22]. This is due to the lower flux densities used in this study and the greater distance between the magnetic particles in the samples when the samples are undergoing high strain tensile loading compared with shear strain.

Permanent rare earth magnet arrays can produce a higher flux density over the sample volume than iron core electromagnets and have zero power (energy cost) requirements in maintaining the magnetic field. However electromagnets offer the advantage that the magnetic field can be switched on and off during a test without any modification to the test set up or time delay such as that for the removal of the permanent magnets. This allows any variation due to sample manufacture or sample conditions to be eliminated as an effect on the change detected and a direct comparison between field on and off properties can be made.

6 Further Work

It is proposed that further studies will explore the effect of strain and strain amplitude on the MR effect for both cyclic uniaxial and biaxial conditions with an applied magnetic flux.

7 Acknowledgements

References

1.   Gorman, D., et al., *Generating a variable uniform magnetic field suitable for fatigue testing magnetorheological elastomers using the bubble inflation method*, in *Constitutive Models for Rubber VIII*2013, CRC Press. p. 671-675.
2.   Boczkowska, A. and S. Awietjan, *Smart composites of urethane elastomers with carbonyl iron.* Journal of Materials Science, 2009. **44**(15): p. 4104-4111.

3.   Stepanov, G.V., et al., *Effect of a homogeneous magnetic field on the viscoelastic behavior of magnetic elastomers.* Polymer, 2007. **48**(2): p. 488-495.

4.   Varga, Z., G. Filipcsei, and M. Zrínyi, *Magnetic field sensitive functional elastomers with tuneable elastic modulus.* Polymer, 2006. **47**(1): p. 227-233.

5.   Schubert, G. and P. Harrison, *Large-strain behaviour of Magneto-Rheological Elastomers tested under uniaxial compression and tension, and pure shear deformations.* Polymer Testing, 2015. **42**: p. 122-134.

6.   Gorman, D., et al., *Creating a uniform magnetic field for the equi-biaxial physical testing of magnetorheological elastomers; electromagnet design, development and testing.* Constitutive Models for Rubber VII, 2011: p. 403.

7.   Bica, I., *Compressibility modulus and principal deformations in magneto-rheological elastomer: The effect of the magnetic field.* Journal of Industrial and Engineering Chemistry, 2009. **15**(6): p. 773-776.

8.   Boczkowska, A., et al. *Effect of the processing conditions on the microstructure of urethane magnetorheological elastomers*. 2006. San Diego, CA, USA: SPIE.

9.   Boczkowska, A., et al., *Image analysis of the microstructure of magnetorheological elastomers.* Journal of Materials Science, 2009. **44**(12): p. 3135-3140.

10.   Chen, L., et al., *Investigation on magnetorheological elastomers based on natural rubber.* Journal of Materials Science, 2007. **42**(14): p. 5483-5489.

11.   Deng, H.X. and X.L. Gong, *Adaptive Tuned Vibration Absorber based on Magnetorheological Elastomer.* Journal of Intelligent Material Systems and Structures, 2007. **18**(12): p. 1205-1210.

12.   GONG, X.L., L. CHEN, and J.F. LI, *STUDY OF UTILIZABLE MAGNETORHEOLOGICAL ELASTOMERS.* International Journal of Modern Physics B, 2007. **21**(28n29): p. 4875-4882.

13.   Coey, J.M.D., *Permanent Magnet Applications.* ChemInform, 2003. **34**(11): p. no-no.

14.   Meeker, D., *FEMM*: http://www.femm.info/wiki/HomePage.

15.   Hills, B.P., K.M. Wright, and D.G. Gillies, *A low-field, low-cost Halbach magnet array for open-access NMR.* Journal of Magnetic Resonance, 2005. **175**(2): p. 336-339.

16.   Murphy, N., et al. *Determining multiaxial fatigue in elastomers using bubble inflation*. in *CONSTITUTIVE MODELS FOR RUBBER-PROCEEDINGS-*. 2005. Balkema.

17.   Murphy, N., J. Hanley, and S. Jerrams, *A method of real-time bi-axial strain control in fatigue testing of elastomers.* Constitutive Models for Rubber VII, 2011: p. 409.

18.   Johnson, M., et al., *The equi-biaxial fatigue characteristics of EPDM under true (Cauchy) stress control conditions.* Constitutive Models for Rubber VIII, 2013: p. 383.

19.   Maxwell, J.C., *On Physical Lines of Force*1862.

20.   Mullins, L. and N. Tobin, *Stress softening in rubber vulcanizates. Part I. Use of a strain amplification factor to describe the elastic behavior of filler-reinforced vulcanized rubber.* Journal of Applied Polymer Science, 1965. **9**(9): p. 2993-3009.

21.   *McIntyre, J. (2013) Characterisation and Optimisation of Magnetorheological Elastomers. A thesis submitted in partial fulfilment of the Institute's requirements for the degree of Doctor of Philosophy Dublin Institute of Technology and Warsaw University, November 2013.*

22.   McIntyre J, Jerrmans S, and Alshuth T, *Magnetorheological Elastomers Developemt of MREs for automotive applications.* Tire Technology International, 2013: p. 42-45.